S_N2 Reaction at Neutral Nitrogen: Transition State Geometries and Intrinsic Barriers

Michael Bühl and Henry F. Schaefer III*

Contribution from the Center of Computational Quantum Chemistry, University of Georgia, Athens, Georgia 30602

Received February 16, 1993®

Abstract: The reactants, ion–dipole complexes, transition states, and products for the nucleophilic displacement reactions $X^- + H_2NY \rightarrow H_2NX + Y^-$ have been optimized at the ab initio DZP+/SCF level of theory for X, Y = F, Cl, OH, CN, and H. The intrinsic barriers for the degenerate reactions (25.3, 22.9, 38.8, and 75.3 kcal/mol for X = Y = F, Cl, OH, and CN, respectively) are larger than the corresponding values for carbon species. The intrinsic barriers $\Delta E^{\ddagger}_{X,Y}$ correlate with the degree of the N–X and N–Y bond elongations in the transition structures. Both intrinsic and overall barriers can be interpreted with the aid of Marcus theory. Deprotonation, rather than substitution, may be an important side reaction for some NH acidic compounds. Alkyl substitution at the central nitrogen increases the intrinsic barrier, cf. $\Delta E^{\ddagger} = 35.6$ kcal/mol for the $F^- + Me_2NF$ identity reaction.

Introduction

The S_N2 nucleophilic displacement at carbon is probably the most intensively studied of all chemical reactions, both experimentally[1–3] and theoretically.[4–6] Despite the intriguing analogy, other elements as central atoms have received much less attention.[7–10] Interest in nucleophilic displacement reactions at nitrogen[8] has recently been renewed. Model reactions of ultimate carcinogens of aromatic amines with bionucleophiles have been shown to follow an S_N2 mechanism.[9] Experimental evidence for a classical S_N2 transition state involving nitrogen (**1**) has been given by means of double labeling experiments.[10]

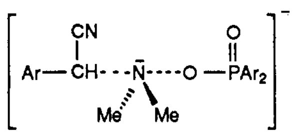

1

Our preliminary communication[11] established a viable pathway for the model reaction

$$F^- + H_2NF \rightarrow \underset{\mathbf{2a}}{F^-{\cdot}H_2NF} \xrightarrow{\underset{\mathbf{2b}}{[F\text{–}NH_2\text{–}F]^{-\ddagger}}} \underset{\mathbf{2a'}}{FNH_2{\cdot}F^-} \rightarrow H_2NF + F^- \quad (1)$$

After formation of an ion–dipole complex (**2a**), the displacement reaction proceeds through a C_{2v} symmetric transition state (**2b**) with one imaginary vibrational frequency. We now report ab initio MO calculations for the general reaction

$$X^- + H_2NY \rightarrow \underset{\mathbf{a}}{X^-{\cdot}H_2NY} \xrightarrow{\underset{\mathbf{b}}{[X\text{–}NH_2\text{–}Y]^{-\ddagger}}} \underset{\mathbf{c}}{XNH_2{\cdot}Y^-} \rightarrow H_2NX + Y^- \quad (2)$$

2: X, Y = F
3: X, Y =Cl
4: X, Y = OH
5: X, Y = CN
6: X, Y = H
7: X = F, Y = Cl
8: X = OH, Y = F
9: X = OH, Y = Cl
10: X = CN, Y = Cl
11: X = F, Y = H

involving other leaving groups and nucleophiles. Comparison with the corresponding reactions at a carbon center reveals that S_N2 barriers are inherently larger for nitrogen than they are for

---

® Abstract published in *Advance ACS Abstracts,* September 1, 1993.

[1] See e.g.: (a) Lowry, T. H.; Richardson, K. S. *Mechanism and Theory in Organic Chemistry,* 3rd ed.; Harper and Row: New York, 1987. (b) Ingold, C. K. *Structure and Mechanism in Organic Chemistry,* 2nd ed.; Cornell University Press: Ithaca, 1969.

[2] (a) Wladkowski, B. D.; Lim, K. F.; Allen, W. D.; Brauman, J. I. *J. Am. Chem. Soc.* **1992,** *114,* 9136. (b) Graul, S. T.; Bowers, M. T. *J. Am. Chem. Soc.* **1991,** *113,* 9696. (c) Yen, Y. F.; Cross, R. J.; Saunders, M. *J. Am. Chem. Soc.* **1991,** *113,* 5563. (d) De Puy, C. H.; Gronert, S.; Mullin, A.; Bierbaum, V. M. *J. Am. Chem. Soc.* **1990,** *112,* 8650 and references cited therein.

[3] (a) Riveros, J. M.; José, S. M.; Takashima, K. *Adv. Phys. Org. Chem.* **1985,** *21,* 197. (b) Caldwell, G.; Magnera, T. F.; Kebarle, P. *J. Am. Chem. Soc.* **1984,** *106,* 959. (c) Tamaka, K.; Mackay, G. I.; Payzant, J. D.; Bohme, D. K. *Can. J. Chem.* **1976,** *54,* 1643.

[4] Shaik, S. S.; Schlegel, H. B.; Wolfe, S. *Theoretical Aspects of Physical Organic Chemistry: The S_N2 Mechanism*; Wiley: New York, 1992. For recent ab initio studies see: (a) Jensen, F. *Chem. Phys. Lett.* **1992,** *196,* 368. (b) Vetter, R.; Zülicke, L. *J. Am. Chem. Soc.* **1990,** *112,* 5136. (c) Shi, Z.; Boyd, R. J. *J. Am. Chem. Soc.* **1990,** *112,* 6789. (d) Shaik, S. S.; Schlegel, H. B.; Wolfe, S. *J. Chem. Soc., Chem. Commun.* **1988,** 1322.

[5] For multidimensional potential energy surfaces see: (a) Vande Linde, S. R.; Hase, W. L. *J. Phys. Chem.* **1990,** *94,* 2778. (b) Tucker, S. C.; Truhlar, D. G. *J. Am. Chem. Soc.* **1990,** *112,* 3338.

[6] (a) Bianco, R.; Miertus, S.; Persico, M.; Tomasi, J. *Chem. Phys.* **1992,** *168,* 281. (b) Gao, J. *J. Am. Chem. Soc.* **1991,** *113,* 7769. (c) Tucker, S. C.; Truhlar, D. G. *J. Am. Chem. Soc.* **1990,** *112,* 3347. (d) Chandrasekhar, J.; Jorgensen, W. L. *J. Am. Chem. Soc.* **1985,** *107,* 2974. (e) For a semiempirical study see: Ford, G. P.; Wang, B. *J. Am. Chem. Soc.* **1992,** *114,* 10563.

[7] (a) For recent work on phosphorus see: Li, P.; Beak, P. *J. Am. Chem. Soc.* **1992,** *114,* 9206. (b) For bromine see: Beak, P.; Allen, D. J. *J. Am. Chem. Soc.* **1992,** *114,* 3420. (c) Review: Beak, P. *Acc. Chem. Res.* **1992,** *25,* 215. (d) For a review on silicon see: Damrauer, R.; Bowie, J. H.; Shelton, J. C. *Acc. Chem. Res.* **1987,** *20,* 127.

[8] For earlier general studies see e.g.: (a) Krueger, J. H.; Sudbury, B. A.; Blanchet, P. F. *J. Am. Chem. Soc.* **1974,** *96,* 5733. (b) Sudbury, B. A.; Krueger, J. H. *Inorg. Chem.* **1974,** *13,* 1974. (c) Heesing, A.; Steinkamp, H. *Tetrahedron Lett.* **1981,** 3827. (c) Heesing, A.; Steinkamp, H. *Chem. Ber.* **1982,** *115,* 2894.

[9] (a) Ulbrich, R.; Famulok, M.; Bosold, F.; Boche, G. *Tetrahedron Lett.* **1990,** *31,* 1689. (b) Helmick, J. S.; Martin, K. A.; Heinrich, J. L.; Novak, M. *J. Am. Chem. Soc.* **1991,** *113,* 3459. (c) Novak, M.; Martin, K. A.; Heinrich, J. L. *J. Org. Chem.* **1989,** *54,* 5430. (d) Famulok, M.; Boche, G. *Angew. Chem., Int. Ed. Engl.* **1989,** *28,* 337.

[10] Beak, P.; Li, J. *J. Am. Chem. Soc.* **1991,** *113,* 2796.

[11] Bühl, M.; Schaefer, H. F. *J. Am. Chem. Soc.* **1993,** *115,* 364.

0002-7863/93/1515-9143$04.00/0

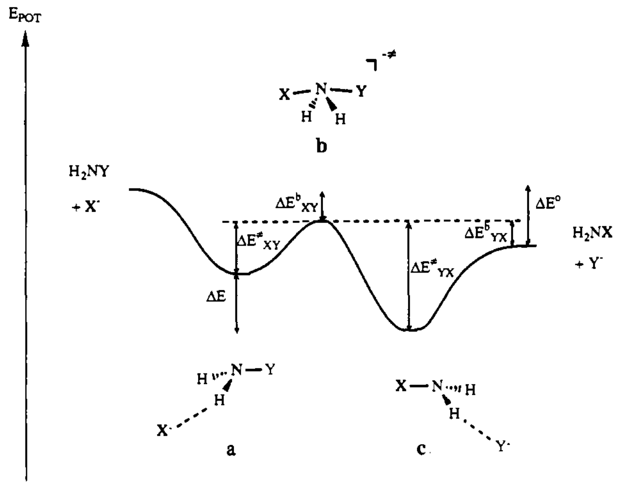

Figure 1. Reaction coordinate for the gas-phase displacement reaction $X^- + H_2NY \rightarrow Y^- + H_2NX$ and definitions of the quantities for eqs 5 and 6.

carbon. Both intrinsic and overall barriers for the unsymmetric cases **7–11** are shown to be reliably predicted by Marcus theory.

Methods

All geometries have been fully optimized[12] in the given symmetry with the self-consistent-field (SCF) method employing a standard double ζ plus polarization (DZP) basis set consisting of the Huzinaga–Dunning (9s5p1d/4s2p1d) basis[13] on C ($\alpha_d = 0.75$), N ($\alpha_d = 0.8$), O ($\alpha_d = 0.85$), and F ($\alpha_d = 1.0$), the (11s7p1d/6s4p1d) basis on Cl ($\alpha_d = 0.75$), and the (4s1p/2s1p) basis on H ($\alpha_p = 0.75$). The nature of each stationary point was probed by harmonic vibrational frequency evaluations at that level; minima and transition states are characterized by zero and one imaginary frequencies, respectively. The geometries were then reoptimized employing the DZP+ basis set, which is the same as DZP augmented with a set of diffuse s- and p-functions on C ($\alpha_s = 0.045$, $\alpha_p = 0.034$), N ($\alpha_s = 0.062$, $\alpha_p = 0.048$), O ($\alpha_s = 0.079$, $\alpha_p = 0.059$), F ($\alpha_s = 0.089$, $\alpha_p = 0.074$), and Cl ($\alpha_s = 0.050$, $\alpha_p = 0.049$).[14] In the cases of X or Y = H, the DZP++ basis set was used, which is the same as DZP+, augmented with a diffuse s-function on H ($\alpha_s = 0.048$).[15] Unless otherwise noted, energies are reported at the DZP+/SCF level.

Results and Discussion

The gas-phase reaction profile for the concerted S_N2 reaction at nitrogen, as depicted in Figure 1, is fully equivalent to the reaction profile of the corresponding reaction 3 at carbon.

$$X^- + H_3CY \rightarrow X^-{\cdot}H_3CY \xrightarrow{[X\text{–}CH_3\text{–}Y]^{-\neq}} XCH_3{\cdot}Y^- \rightarrow H_3CX + Y^- \quad (3)$$

In contrast to the more symmetric carbon analogues, all ion–dipole complexes **a** and **c** involving nitrogen are characterized by a single, essentially linear NH···X hydrogen bond and possess C_1 symmetry. However, the same structural feature, i.e. a single CH···X contact, has been found in $Cl^-{\cdot}H_2C(CN)$–Cl,[2a] a complex bearing an additional electron-withdrawing substituent at carbon.

The intrinsic barrier for reaction 1, i.e. the relative energy of **2b** with respect to **2a**, has been shown to be quite insensitive to the level of theory employed (e.g. 25.3 and 24.0 kcal/mol at DZP+/SCF and TZP+/CISD, respectively).[11] Therefore, the rather modest DZP+/SCF level, which should give reliable results, was employed throughout this study. In addition, it is known for the carbon analogues that electron correlation has a large effect on geometries, but not on energies.[4c] Computed energies and selected geometrical parameters of the various stationary points **a–c** are presented in Tables I and II, respectively. Relative energies, e.g. intrinsic and overall barriers, $\Delta E^{\neq}_{X,Y}$ and $\Delta E^b_{X,Y}$, respectively, are given in Table III.

Table I. Absolute Energies (–au) for Complexes and Transition States **2–12**, as Well as for Reactants and Products. As Noted, Several Purported Stationary Points Collapse

compd	symmetry	DZP/SCF	ZPE[a]	DZP+/SCF
(**2a**) $F^-{\cdot}H_2NF$	C_1	254.47403	18.6(0)	254.49659
(**2b**) F–NH_2F–F^-	C_{2v}	254.43459	18.7(1)	254.45626
(**3a**) $Cl^-{\cdot}H_2NCl$	C_1	974.58317	18.4(0)	974.61122
(**3b**) Cl–NH_2–Cl^-	C_{2v}	974.55034	17.6(1)	974.57468
(**4a**) $HO^-{\cdot}H_2NOH$	C_1	206.43296	34.2(0)	206.45836
(**4b**) HO–NH_2–OH^-	C_{2v}	206.37335	33.4(1)	206.39645
(**5a**) $NC^-{\cdot}H_2NCN$	C_1	240.29101	27.6(0)	240.30398
(**5b**) NC–NH_2–CN^-	C_{2v}	240.17301	26.5(1)	240.18392
(**6a**) $H^-{\cdot}H_3N$	C_s	56.64872	24.4(0)	56.70780[b]
(**6b**) H–NH_2–H^-	C_{2v}	56.70780	21.7(1)	$\rightarrow T_d$
(**7a**) $Cl^-{\cdot}H_2NF$	C_1	614.52048	17.1(0)	614.54337
(**7b**) Cl–NH_2–F^-	C_s	614.48857	17.9(1)	614.51216
(**7c**) $F^-{\cdot}H_2NCl$	C_1	614.53384	19.5(0)	614.56707
(**8a**) $HO^-{\cdot}H_2NF$	C_1	230.43174	24.7(0)	230.45476
(**8b**) HO–NH_2–F^-	C_s	230.39586	25.5(1)	230.41804
(**8c**) $F^-{\cdot}H_2NOH$	C_1	230.47629	27.9(0)	230.50057
(**9a**) $HO^-{\cdot}H_2NCl$	C_1	$\rightarrow HOH{\cdot}NHCl^-$	24.2(0)[c]	590.50182
(**9b**) HO–NH_2–Cl^-	C_1[d]	590.45408	24.7(1)	590.47886
(**9c**) $Cl^-{\cdot}H_2NOH$	C_1	590.54658	28.2(0)	590.57508
(**10a**) $NC^-{\cdot}H_2NCl$	C_1	607.38893	22.5(0)	607.40483
(**10b**) NC–NH_2–Cl^-	C_s	607.35891	21.8(1)	607.37554
(**10c**) $Cl^-{\cdot}H_2NCN$	C_1	607.48562	23.7(0)	607.51009
(**11a**) $H^-{\cdot}H_2NF$	C_1	$\rightarrow H_2{\cdot}NHF^-$	20.1(0)[c]	155.52122[b]
(**11b**) H–NH_2–F^-	C_s	155.45843	19.4(1)	155.49999[b]
(**11c**) $F^-{\cdot}H_3N$	C_s	155.65374	24.1(0)	155.67792[b]
(**12a**) $F^-{\cdot}Me_2NF$	C_s	332.54458	56.2(0)	332.56716
(**12b**) F–NMe_2–F^-	C_2	332.49081	55.5(1)	332.51047
H_2NF	C_s	155.00757	19.0(0)	155.01089[e]
H_2NCl	C_s	515.05139	18.0(0)	515.05544
H_2NOH	C_s	131.02506	27.7(0)	131.02845
H_2NCN	C_s	147.94066	23.2(0)	147.94393
NH_3	C_{3v}	56.20901	23.1(0)	56.21108[b]
Me_2NF	C_s	233.08960	56.4(0)	233.09308
F^-	K_h	99.41406		99.44565
Cl^-	K_h	459.50320		459.53417
OH^-	$C_{\infty v}$	75.37066	5.6(0)	75.40354
CN^-	$C_{\infty v}$	92.31099	3.3(0)	92.32684
H^-	K_h	0.40525		0.48565[b]

[a] Zero-point energy (kcal/mol), DZP/SCF level, unscaled. The number of imaginary vibrational frequencies is given in parentheses. For the transition structures, the vibration of the imaginary frequency corresponds to the displacement of X^- by Y^-, or vice versa. [b] DZP++/SCF level. [c] DZP+/SCF level. [d] Unlike the C_s symmetric transition structures **7b**, **8b**, **10b**, and **11b**, **9b** lacks all symmetry; a C_s symmetric stationary point has a smaller second imaginary frequency, both at DZP/SCF and DZP+/SCF levels. [e] DZP++/SCF: 155.01093.

The transition structure for the $H^- + H_3N$ displacement reaction (**6b**, C_{2v} symmetry) is a stationary point only at the DZP/SCF level of theory. Optimization at the DZP++/SCF level, i.e. with inclusion of diffuse functions, affords NH_4^- in T_d symmetry, which has been shown to be a minimum on the potential energy surface (PES).[16] Obviously, the reaction profile depicted in Figure 1 exists only at the DZP/SCF level (among methods used here) for this particular system (**6**) and is an artifact due to the inadequacy of that level. However, the DZP/SCF values have been included in Tables I–III for comparison with the carbon analogues and for the Marcus-type equations below.

Intrinsic Barriers. The intrinsic (central) barriers for the identity reactions, i.e. X = Y, are considerably larger in the case of the nitrogen species **2–6** than for the carbon analogues (values

---

[12] All calculations were performed with PSI 2.0, 1991, PSITECH Inc., Watkinsville, Georgia.

[13] (a) Huzinaga, S. *J. Chem. Phys.* **1965**, *42*, 1293. (b) Dunning, T. H., Jr. *J. Chem. Phys.* **1970**, *53*, 2823; *ibid.* **1971**, *55*, 716.

[14] Cf.: Dunning, T. H., Jr.; Hay, P. J. In *Modern Theoretical Chemistry*; Schaefer, H. F., Ed.; Plenum Press: New York, 1977; Vol. 3.

[15] Cf.: Janssen, C. L.; Allen, W. D.; Schaefer, H. F., Bowman, J. M. *Chem. Phys. Lett.* **1986**, *131*, 352.

[16] (a) Gutowski, M.; Simons, J. *J. Chem. Phys.* **1990**, *93*, 3874. (b) Ortiz, J. V. *J. Phys. Chem.* **1990**, *94*, 4762. (c) Cardy, H.; Larrieu, C.; Dargelos, A. *Chem. Phys. Lett.* **1986**, *131*, 507.

Table II. Selected Geometrical Parameters (angstroms and degrees) for Ion–Dipole Complexes (**a** and **c**) and for Transition Structures (**b**) Optimized at the DZP+/SCF Level

	parameter								
	a			**b**			**c**		
X, Y	N–Y	N–H(X)[a]	H–X	N–X	N–Y	X–N–Y	N–X	N–H(Y)[a]	H–Y
2 F, F	1.418	1.050	1.553	1.842		161.4			
3 Cl, Cl	1.745	1.016	2.386	2.295		165.7			
4 OH, OH	1.425	1.038	1.731	1.914		163.6			
5 CN, CN	1.335	1.030	2.015	2.016		171.9			
6 H, H[b]	1.006	1.015	2.259	1.612[c]		165.5[c]			
7 F, Cl	1.763	1.070	1.468	1.978	2.169	161.2	1.402	1.011	2.500
8 OH, F	1.419	1.051	1.638	2.010	1.768	163.7	1.424	1.037	1.640
9 OH, Cl	1.770	1.092	1.499	2.163	2.078	158.5	1.413	1.010	2.545
10 CN, Cl	1.744	1.021	2.151	2.213	2.145	167.6	1.336	1.020	2.255
11 H, F[b]	1.407	1.022	1.933	1.942	1.675	162.5	1.006	1.033	1.734

[a] N–H bond length involved in the hydrogen bridge; in almost all cases, the other N–H bond length is between 1.004 and 1.006 Å. [b] DZP++/SCF level. [c] DZP/SCF level.

Table III. Reaction Energies, Overall and Intrinsic Barriers (kcal/mol, DZP+/SCF Level), and Percentage N–X and N–Y Transition-Structure Bond Elongations

X, Y	ΔE°	ΔE	$\Delta E^{b}{}_{X,Y}$	$\Delta E^{b}{}_{Y,X}$	$\Delta E^{\ddagger}{}_{X,Y}$	$\Delta E^{\ddagger}{}_{Y,X}$	% NX	% NY
2 F, F			0.2		25.3		30.2	
3 Cl, Cl			9.4		22.9		31.5	
4 OH, OH			22.3		38.8		34.3	
5 CN, CN			54.5		75.3		51.0	
6 H, H[a]			70.1		77.0		60.2	
7 F, Cl	−27.6	−14.8	−6.9	20.7	19.7	34.5	23.0	40.7
8 OH, F	−37.5	−28.7	−2.3	35.2	23.1	51.8	24.6	41.1
9 OH, Cl	−65.1	−46.0	−12.5	52.6	14.4	60.4	17.4	53.1
10 CN, Cl	−60.1	−66.8	4.2	64.3	17.6	84.4	23.0	65.6
11 H, F	−100.5	−98.3	−2.1	98.4	13.4	111.7	19.0	93.0

[a] DZP level.

in parentheses), namely 25.3 (18.6),[17] 22.9 (15.5),[17] 38.8 (21.2),[18] 75.3 (43.8),[18] and 77.0 (63.1)[17] kcal/mol, for X, Y = F, Cl, OH, CN, and H, respectively. This is in line with the intuitive expectation that the approach of a negatively charged nucleophile toward the more electronegative nitrogen should be less favorable. The trend, however, is the same for both elements, i.e. $Cl^- < F^- < OH^- < CN^-$ ($< H^-$). For the unsymmetric reactions, the intrinsic barriers $\Delta E^{\ddagger}{}_{X,Y}$ span the range between ca. 14 and 23 kcal/mol. Due to some very large reaction energies, ΔE, the barriers for the reverse reactions, $\Delta E^{\ddagger}{}_{Y,X}$, can be much higher, between ca. 35 and 112 kcal/mol (Table III).

Transition State Geometries. For S_N2 reactions at carbon, the "looseness" of the transition state correlates with the magnitude of the central barrier, i.e. a higher barrier is associated with a larger deformation (stretching) of the C–X bond in the transition structure.[4] The question is, does a similar relationship exist between $\Delta E^{\ddagger}{}_{X,Y}$ of the nitrogen species and the transition state geometries in Table II? Shaik, Schlegel, and Wolfe[4d] have defined a percentage C–X bond elongation that can easily be transferred to a percentage N–X bond elongation in nitrogen species:

$$\%\,\mathrm{NX}^{\ddagger} = 100(d^{\ddagger}{}_{\mathrm{NX}} - d^{0}{}_{\mathrm{NX}})/d^{0}{}_{\mathrm{NX}} \qquad (4a)$$

$$\%\,\mathrm{NY}^{\ddagger} = 100(d^{\ddagger}{}_{\mathrm{NY}} - d^{0}{}_{\mathrm{NY}})/d^{0}{}_{\mathrm{NY}} \qquad (4b)$$

where $d^{\ddagger}$ and d^{0} are the bond lengths in transition states (**b**) and in ion–dipole complexes (**a** or **c**), respectively.[19] As can be seen from the plot in Figure 2, there is a roughly linear relationship between % $\mathrm{NX}^{\ddagger}$ and $\Delta E^{\ddagger}$. As is the case with carbon, the higher the S_N2 barrier, the more extensive is the bond cleavage of the leaving group in the transition state.

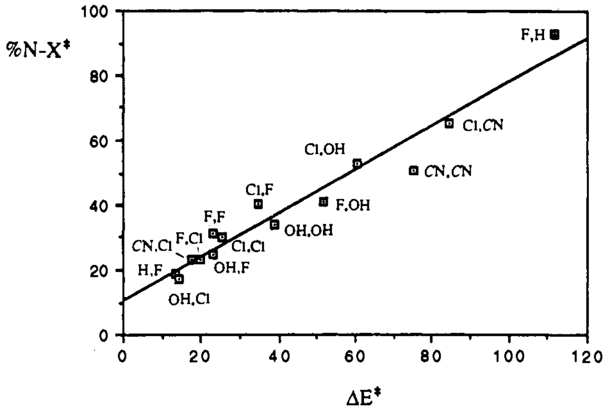

Figure 2. Plot of % NX‡ versus the central barrier height (kcal/mol, DZP+/SCF level) for the reaction $X^- + H_2NY \rightarrow Y^- + H_2NX$. Data points are labeled X, Y (italic C indicates the site of attachment).

Rate–Equilibrium Relationships. Marcus theory[20] has been successfully applied, among other reactions, to the interpretation of gas-phase S_N2 reactions at carbon. The Marcus equation

$$\Delta E^{\ddagger}{}_{X,Y} = {}^{1}/_{2}(\Delta E^{\ddagger}{}_{X,X} + \Delta E^{\ddagger}{}_{Y,Y}) + {}^{1}/_{2}\Delta E + [(\Delta E)^2/8(\Delta E^{\ddagger}{}_{X,X} + \Delta E^{\ddagger}{}_{Y,Y})] \qquad (5)$$

relates the intrinsic barrier height of an unsymmetric displacement, $\Delta E^{\ddagger}{}_{X,Y}$, to the intrinsic barriers of the degenerate reactions, $\Delta E^{\ddagger}{}_{X,X}$ and $\Delta E^{\ddagger}{}_{Y,Y}$, and to the energy change ΔE. The range of intrinsic barriers computed for nitrogen species is quite large, ca. 100 kcal/mol (Table III). As illustrated in Figure 3, a plot of barriers $\Delta E^{\ddagger}{}_{X,Y}$ calculated according to eq 5 versus the ab initio data from Table III, the barriers predicted by Marcus theory are within a few kcal/mol of the "actual", ab initio computed values.

---

(17) 6-31+G*/SCF values from ref 4c. The 6-31+G*/MP2 values are 12.9, 17.4, and 55.2 kcal/mol, respectively, for X, Y = F, Cl, and H (6-31++G** basis for X, Y = H).

(18) 4-31G level: Wolfe, S.; Mitchell, D. J.; Schlegel, H. B. *J. Am. Chem. Soc.* **1981**, *103*, 7692, 7694.

(19) Even if the individual computed bond lengths may change at higher levels of theory (cf. refs 4c and 11), the general trend in the % NX‡ values should be reliable.

(20) (a) Marcus, R. A. *Annu. Rev. Phys. Chem.* **1964**, *15*, 155 and references therein. (b) Marcus, R. A.; Hase, W. L.; Swamy, K. N. *J. Phys. Chem.* **1984**, *88*, 6717. See also: (c) Sutin, N. *Annu. Rev. Phys. Chem.* **1966**, *17*, 119.

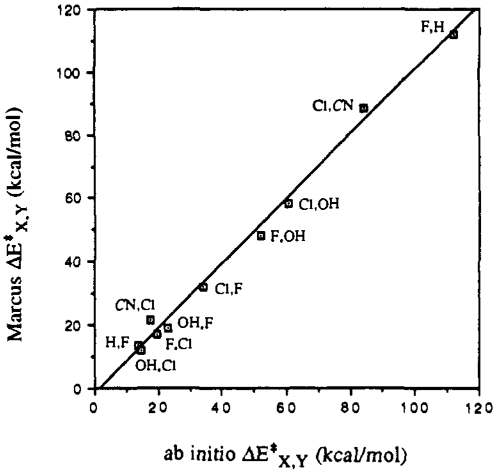

Figure 3. Plot of $\Delta E^{\ddagger}_{X,Y}$ from eq 5 versus the same quantity obtained directly from the energy differences between ion–dipole complexes **a** or **c** and transition structures **b** (DZP+/SCF ab initio level).

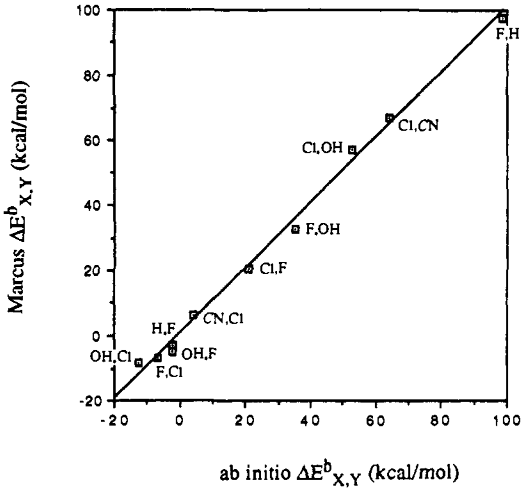

Figure 4. Plot $\Delta E^{b}_{X,Y}$ from eq 6 versus the same quantity obtained directly from the energy differences between $X^- + H_2NY$ and transition structures **b** (DZP+/SCF ab initio level).

Wolfe, Mitchell, and Schlegel[18] derived a similar Marcus-type equation for the overall barrier $\Delta E^{b}_{X,Y}$, (i.e. with respect to the isolated reactants):

$$\Delta E^{b}_{X,Y} \approx {}^{1}/_{2}(\Delta E^{b}_{X,X} + \Delta E^{b}_{Y,Y}) + {}^{1}/_{2}\Delta E^{0} + [(\Delta E^{0})^2/8(\Delta E^{\ddagger}_{X,X} + \Delta E^{\ddagger}_{Y,Y})] \quad (6)$$

This equation permits the prediction of the experimentally more accessible quantity $\Delta E^{b}_{X,Y}$ from data of the corresponding identity reactions. Figure 4, a plot of $\Delta E^{b}_{X,Y}$ deduced by eq 6 versus $\Delta E^{b}_{X,Y}$ computed ab initio (Table III), illustrates the applicability of eq 6 to the S_N2 reaction at nitrogen. Again, the ab initio barriers are reproduced by Marcus theory within a few kcal/mol, on a scale of more than 100 kcal/mol. It is especially noteworthy that the "negative barriers" (i.e. transition states **b** lower in energy than reactants) in the forward reactions of systems **7**, **8**, **9**, and **11** are predicted correctly by eq 6, even though all degenerate reactions, i.e. systems **2–6**, have positive, computed overall barriers.[21]

In summary, the S_N2 reaction at nitrogen shows a close resemblance to its well-known carbon counterpart. Both reactions proceed through transition states, the "looseness" of which is related to the degree of bond breaking and bond forming as reflected in the bond elongations in the transition structures. Also, both reactions can be interpreted with the aid of Marcus theory. It is our hope that these results may be useful in future experimental studies of the S_N2 reaction at nitrogen, particularly in the gas phase.

Proton Transfer. To our knowledge, the only mechanistic studies on one of the **2–11** systems have been reported for the $NH_2Cl + OH^-$ reaction (system **9**).[22,23] The conversion of chloramine to hydroxylamine in basic solution is thought to be one of the main steps in the Raschig process[24] for the synthesis of hydrazine. From the rate law[22] and from a negative volume of activation,[23] the bimolecular S_N2 process was deduced as the reaction mechanism in solution. This is consistent with our findings for the gas-phase reaction

$$HO^- + H_2NCl \rightarrow NH_2OH + Cl^- \quad (7)$$

for which a large driving force (reaction energy $\Delta E^0 = -65$ kcal/mol) and a relatively small intrinsic barrier ($\Delta E^{\ddagger}_{OH,Cl} = 14.4$ kcal/mol) are computed. At the DZP/SCF level, however, the ion–dipole complex $HO^-{\cdot}H_2NCl$ (**9a**) is not a minimum but optimizes to the $HOH{\cdot}NHCl^-$ complex, i.e. proton transfer occurs, apparently without any barrier. On the other hand, **9a** is a true minimum at the DZP+/SCF level of theory, demonstrating that there exists in fact a barrier for this process. However, the exothermicity of the deprotonation reaction

$$HO^- + H_2NCl \rightarrow H_2O + NHCl^- \qquad \Delta E = -16.9 \text{ kcal/mol} \quad (8)$$

as well as the significantly elongated NH bond involved in the hydrogen bond of **9a** (1.092 Å, Table II) indicate that this barrier may be small. Hence, it appears that deprotonation can be an important competitive reaction to the S_N2 displacement.[25] A more detailed study of this reaction channel, however, is beyond the scope of this paper.

Among the systems of this study, the $CN^- + H_2NCl$ displacement reaction (system **10**) is perhaps the best "candidate" for observation in the gas phase, as judged from energetic considerations: Besides a large reaction exothermicity, $\Delta E = -60.1$ kcal/mol, and a relatively small intrinsic barrier, $\Delta E^{\ddagger}_{CN,Cl} = 17.6$ kcal/mol, deprotonation of both reactant and product is energetically unfavorable:

$$CN^- + H_2NCl \rightarrow HCN + NHCl^- \qquad \Delta E = 31.9 \text{ kcal/mol} \quad (9a)$$

$$Cl^- + H_2NCN \rightarrow HCl + NHCN^- \qquad \Delta E = 30.9 \text{ kcal/mol} \quad (9b)$$

The overall barrier, $\Delta E^{b}_{CN,Cl} = 4.2$ kcal/mol, should be small enough for the reaction to proceed with sufficient efficiency. Predictions of rate constants, however, would have to include multidimensional potential energy surfaces and advanced dynamical methods such as variational transition state theory.[5]

Steric Effects. The experimental evidence for the "classical" S_N2 transition state involving nitrogen (**1**) has been given for a *N,N*-dimethyl substrate.[10] For carbon systems, increasing C-alkyl substitution has been shown to decrease the S_N2 reaction rates, and to increase the intrinsic barriers;[3a,4a] e.g., in the $Cl^- + R\text{-}Cl$ system going from $R = CH_3$ to R = i-Pr results in a change of the intrinsic barrier from 15.3 to 21.5 kcal/mol (6-31G*/SCF level).[26]

---

[21] However, at higher levels of theory, **2b** is more stable than the reactants, e.g. by 2.9 kcal/mol at the TZP+/CISD level, cf. ref 11.

[22] Anbar, M.; Yagil, G. *J. Am. Chem. Soc.* **1962**, *84*, 1790.

[23] Le Noble, W. N.; *Tetrahedron Lett.* **1966**, *7*, 727.

[24] Review: Fischer, J.; Jander, J. *Z. Anorg. Allg. Chem.* **1961**, *313*, 14.

[25] A referee suggested another reaction channel, namely the nucleophilic displacement of NH_2 via attack at X (recalling that hydrolysis of NCl_3 *in solution* yields ammonia). However, this process appears to be highly unfavorable *in the gas phase*: e.g., the $NH_2F + F^- \rightarrow NH_2^- + F_2$ reaction is computed to be endothermic by 116 kcal/mol (DZP+/SCF level).

[26] Reference 4a; the corresponding barriers at the 6-311+G(2d)/MP2//6-31G*/MP2 level are given as 12.9 and 21.5 kcal/mol, respectively.

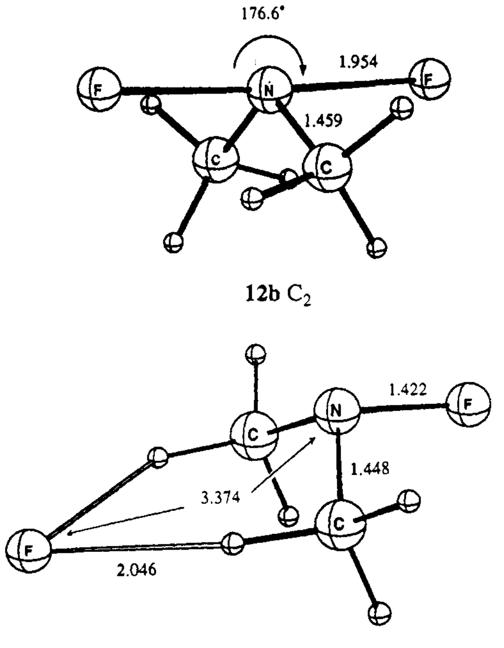

12b C_2

12a C_s

Figure 5. DZP+/SCF optimized geometries for the ion–dipole complex F^-·Me_2NF (**12a**, bottom) and for the transition structure F–NMe_2–F^- (**12b**, top).

In order to investigate similar effects in the case of the nitrogen species, we optimized the F^-·Me_2NF complex (**12a**) and the [F–NMe_2–F]$^{-\ddagger}$ transition state (**12b**, see Figure 5). The minimum **12a** has C_s symmetry with two F^-···HC contacts, in contrast to the parent complex **2a**, where the corresponding symmetrically bridged form is a transition structure for the migration of the F^- from one hydrogen to the other.[11] Transition structure **12** (C_2 symmetry) possesses an almost linear F–N–F arrangement (bending angle 176.6°), with the fluorines bent slightly *away* from the methyl groups. In the parent transition state (**2b**), the fluorines are bent somewhat *toward* the hydrogens (FNF angle 161.4°).

At the DZP+/SCF level, the F^- + Me_2NF complexation energy and the intrinsic barrier $\Delta E^{\ddagger}$ are 17.8 and 35.6 kcal/mol, respectively. The corresponding values for the parent system **2** are 25.1 and 25.3 kcal/mol, respectively (Table III). The increase of $\Delta E^{\ddagger}$ upon dimethyl substitution, ca. 10 kcal/mol, is slightly larger than that of the carbon analogue, ca. 6 kcal/mol, at least at the SCF level.[23] Consistent with the higher barrier of **12** vs **2**, the NF distances in transition structure **12b**, 1.954 Å, are significantly longer than in **2b** (1.842 Å) and correspond to a larger percentage bond elongation according to eq 4 (37.4%, cf. Figure 2).

In contrast to the increase of the central barrier predicted in the gas phase, it is known that "methyl substitution has virtually no effect on the rate of such displacement at nitrogen" in aqueous solution.[23] Apparently, solvent effects attenuate the steric effects of substituents in this case.

Conclusions

The concerted gas-phase S_N2 displacement reactions at carbon and at nitrogen share a number of common characteristics: (i) The first step in each reaction is the formation of an ion–dipole complex. (ii) The magnitude of the intrinsic barrier for the degenerate reactions increases in the order $F^- < Cl^- < OH^- < CN^-$. (iii) The looseness of the transition state, i.e. the degree of elongation of the bond between the central atom and the leaving group, correlates with the intrinsic barrier. (iv) Both intrinsic and overall barriers for unsymmetric reactions are reasonably well described by Marcus theory. (v) Alkyl substitution at the central atom increases the intrinsic barrier.

The main differences between the S_N2 reactions at nitrogen and at carbon are as follows: (i) The ion–dipole complexes of nitrogen species lack all symmetry and are characterized by a single X^-···HN hydrogen bond. (ii) The intrinsic barriers involving nitrogen are larger than those involving carbon, e.g. by up to ca. 80% for X, Y = OH. (iii) For some NH acidic substrates, deprotonation may constitute a competing reaction channel.

Since deprotonation side reactions are energetically unfavorable for the CN^- + H_2NCl reaction, this system might be a suitable candidate for experimental studies in the gas phase.

Direct comparison of our ab initio results to experiments in solution, however, is not possible. For carbon, reaction rates in solution can be smaller by many orders of magnitude than the corresponding rates in the gas phase. The shape of the PES and the height of the central barrier in particular may change significantly upon solvation.[6] Given all the common features of S_N2 reactions at carbon and at nitrogen reported here, we would expect similar solvent effects for reactions involving nitrogen species.

Acknowledgment. This research was supported by the U.S. National Science Foundation, Grant CHE-9216754. M.B. gratefully acknowledges a postdoctoral fellowship of the Deutsche Forschungsgemeinschaft.

Supplementary Material Available: DZP+/SCF optimized Cartesian coordinates for ion–dipole complexes **a** and **c**, and for transition structures **b** (2 pages). Ordering information is given on any current masthead page.